Gustin Solar

Harrisville Township

Exhibit C

Glare Study

June 15, 2026

Rev. September 29, 2026

This Page Intentionally Left Blank

1898 & CO.®
PART OF BURNS McDONNELL

SOLAR GLARE STUDY

CONSUMERS ENERGY COMPANY

GUSTIN SOLAR ENERGY CENTER
192088

September 29, 2026

CONTENTS

1.0 Introduction 1-1

1.1 Study Overview 1-1

1.2 Project Overview 1-1

1.3 Glare Overview 1-1

1.4 Applicable Regulations 1-1

2.0 Modeling Parameters and Inputs 2-1

2.1 Modeling Overview 2-1

2.2 Solar Arrays 2-2

2.3 Receptors 2-2

2.4 Terrain and Existing Vegetation 2-2

2.5 Obstacles 2-3

2.6 Resting Angle 2-3

2.7 Environment 2-3

3.0 Results 3-1

APPENDIX A – GLARE INTENSITY MAP

APPENDIX B – GLARE RESULTS BY RECEPTOR

APPENDIX C – FORGESOLAR METHODOLOGY UPDATE

TABLES

Table 2-1: Parameters for PV Arrays and Modules 2-2

Table 3-1: Summary of Results 3-1

Table B-1: Glare Results by Receptor – Residences B-1

Table B-2: Glare Results by Receptor – Roads B-2

LIST OF ABBREVIATIONS

Abbreviation	Term/Phrase/Name
1898 & Co.	Burns & McDonnell Michigan, Inc. d/b/a/1898 & Co.,
FAA	Federal Aviation Administration
MWac	Megawatt alternating current
Owner	Consumers Energy Company
Project	Gustin Solar Energy Center
Project Site	Location of Project Harrisville Township, Alcona County, Michigan
PV	Photovoltaic
Study	Solar Glare Analysis



1.0 Introduction

1.1 Study Overview

Burns & McDonnell Michigan, Inc. d/b/a 1898 & Co. ("1898 & Co.") prepared a solar glare analysis ("Study") for the Gustin Solar Energy Center (the "Project"), proposed by Consumers Energy Company ("Owner"). The objective of the Study is to estimate the potential for Project solar arrays to direct concentrated glare toward or onto nearby properties or roadways located in Harrisville Township.

1.2 Project Overview

Gustin Solar Energy Center is proposed on land located in Gustin and Harrisville Townships, Alcona County, Michigan, approximately 4.5 miles west of the city of Harrisville. Within Harrisville Township, the Project will generate 94 megawatts alternating current ("MWac").

1.3 Glare Overview

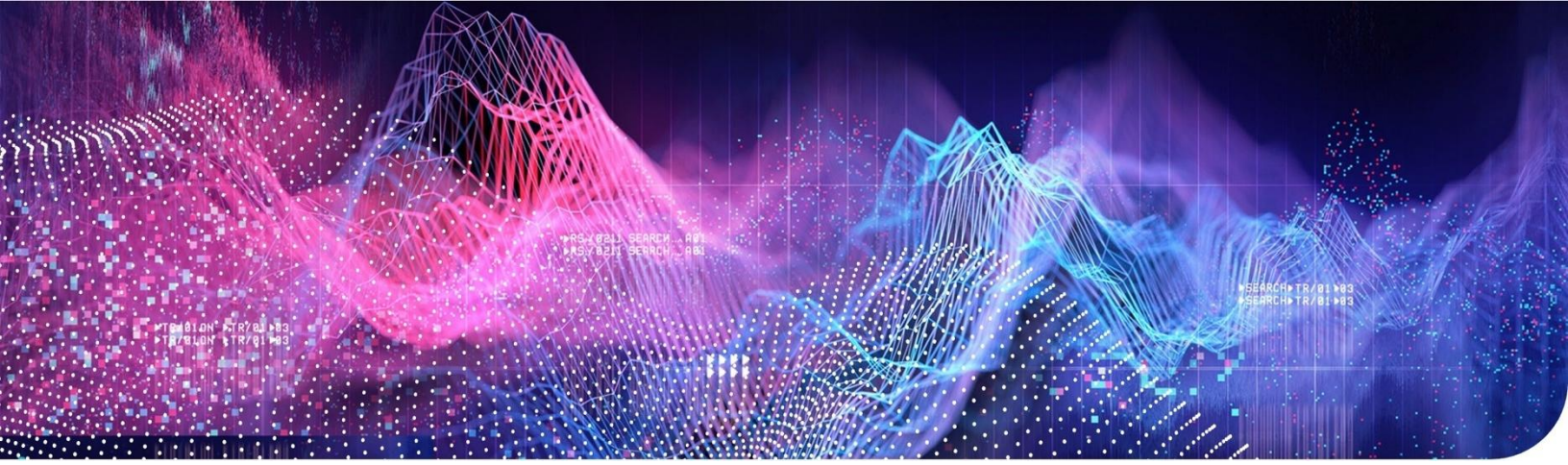
Glare is defined as a continuous source of bright light reflecting off a surface. Concentrated glare occurs when an intense, localized beam of light reflects off a surface in a manner that impedes the ability to see clearly. Solar arrays rarely reflect light in a localized beam. Instead, sun light is reflected over a wide angle that results in the surface appearing bright similar to light reflected off water bodies and wet surfaces. Glare from a solar project only occurs under very specific conditions that are dependent on time of day and year, photovoltaic ("PV") panel position, observer location, and weather conditions. The anti-reflective coatings applied to PV panels help reduce reflective glare but do not eliminate it.

1.4 Applicable Regulations

For purposes of this study, reflective glare is considered consequential if the glare has the potential of causing an after image (reported by ForgeSolar as "yellow" glare), and it does not occur within an hour of sunrise or sunset, and does not emanate from same direction as the sun. Yellow glare that occurs within an hour of sunrise or sunset and that emanates from the same direction as the sun is considered inconsequential because the intensity of the sun is significantly greater than the intensity of the reflective glare of the PV panels, making the impact of glare on the observer negligible as compared to the sun.

Glare associated with solar arrays is not regulated by Alcona County or the State of Michigan. Section 7.31.A.2 of the Harrisville Township Zoning Ordinance provides as follows:

> **Section 7.31.A.2:** *Solar Energy Systems shall be located or placed so that concentrated solar glare shall not be directed toward or onto nearby properties or roadways at any time of the day.*



2.0 Modeling Parameters and Inputs

2.1 Modeling Overview

The potential for reflective glare was modeled for the Project Site using ForgeSolar, a commercially licensed solar glare analysis tool developed by Sandia National Laboratory in conjunction with the Federal Aviation Administration (FAA).

This software models the path of the sun with respect to the orientation of the PV panels during every minute of daylight over a full year. Any light reflected off the arrays is analyzed by receptor location and array block for the entire year. ForgeSolar assigns a color value of “green”, “yellow”, or “red” to the reflected light intensity based on the potential to cause afterimage or permanent damage.

Green Glare	Yellow Glare	Red Glare
Low potential of causing afterimage.	Potential of causing afterimage.	Potential of causing retinal burns only exists for concentrated solar-thermal projects.

The 2026B update to the ForgeSolar software changed how the tilt of the single-axis tracking array is calculated throughout each day. Previously, the tilt of the array would be derived from a vector that does not fully represent the planarized array. The most recent version of ForgeSolar (v3.2.1) derives the tilt of the array more consistently and more accurately from the entire planarized array. The results in Section 3.0 represent the glare calculated with the most recent version of the ForgeSolar software. Appendix C includes the ForgeSolar Methodology Update published in July 2026 and describes the most recent updates to the ForgeSolar software.

The following sections summarize the inputs utilized in the ForgeSolar model for this Study.

2.2 Solar Arrays

The Project was modeled as 34 separate arrays within the ForgeSolar model. (Nine separate arrays are proposed In Harrisville Township.) For each array, the model assessed glare for the entire area encompassed by the polygon, including all the gaps between rows, inverters, and access roads. The parameters for the arrays and PV panels are summarized in Table 2-1. The height of the PV panels above the ground is modeled in ForgeSolar using the centroid of the PV panel, as defined by the ForgeSolar Help Guide. The ForgeSolar software uses the centroid height to calculate the position of the solar panel above the ground throughout the day as the panels track the sun.

Table 2-1: Parameters for PV Arrays and Modules

Array Type	Maximum Tracking Angle (degrees)	Array Azimuth (degrees)	Module Surface Material	Average Height Above Ground (ft)	Ground Coverage Ratio (%)
Single-axis tracking	+/- 52	180	Smooth glass with anti-reflective coating (revised)	5.5	37.2

Glare intensity is partially dependent on the distance between a receptor and the array where glare is occurring and partially dependent on the size of the glare. The Owner-provided layout of the arrays is graphically represented in Appendix A.

2.3 Receptors

The following receptors in Harrisville Township were modeled within Forge Solar:

- 32 buildings were modeled at an observer's eye level at ground-level (6 feet) as "observation points" and at 35 feet, the maximum building height allowed in the Agricultural zoning district as "observation points".
- 8 roads were modeled four feet above ground to replicate the view of the driver of a car and ten feet above ground to replicate the view of a commercial truck driver as "path receptors". The viewing angle applied is 50 degrees from the direction of travel to the left or right (total field of view of 100 degrees) in accordance with FAA research on glare impacts for pilots.

The location of the receptors and roadways were determined using aerial imagery. The location of each receptor is presented graphically in Appendix A, and the coordinates of the buildings are presented in Appendix B.

2.4 Terrain and Existing Vegetation

The ForgeSolar model utilizes topography data to place the arrays and receptors at the proper elevation. The model does not consider any natural features between the arrays and a receptor that may block the glare from being seen at an observation point or path receptor.

Publicly available terrain data was downloaded from the National Elevation Dataset, a product of the United States Geological Survey. The 10-meter resolution digital elevation model was exported as 5-meter intervals for use in the ForgeSolar model. Using this data, elevations were assigned by 1898 & Co. to each vertex of the arrays and each receptor.

2.5 Obstacles

Obstacles located between a receptor and a solar array, such as trees or buildings, can reduce or eliminate the duration and intensity of the glare.

Within the Project Site, there are several substantial forested areas having a width greater than 400 feet. However, to remain conservative, none of the forested areas were modeled in ForgeSolar.

2.6 Resting Angle

The sun's path with respect to each solar array is calculated by the ForgeSolar model to determine the potential for glare during every minute of daylight over a full year. Since the model assumes a flat horizon with no elevation change or obstacles, at low sun angles the model generates erroneous results if the resting angle is set to zero degrees. Thus, a resting angle of five (5) degrees, which is the default setting in ForgeSolar, is utilized for the maximum angle the trackers will rotate backward to during back-tracking. For the analysis, the resting angle does not reach the night-time stow position (zero-degree angle) until the sun is on or below the horizon.

2.7 Environment

Glare only occurs when the sun is shining. The model assumes the sun is always shining, with no consideration given for cloud cover, rainy days, fog, or other similar occurrences that reduce the occurrence or severity of glare. This approach provides a conservative estimate of the amount of time when glare could occur.



3.0 Results

Using the inputs and parameters defined in Section 2.0, the ForgeSolar model calculated the potential for reflected glare to be visible to the identified receptors in Harrisville Township. Table 3-1 summarizes the results. The tables included in Appendix B detail potential glare duration and intensity by receptor, including estimated daily minutes. The maps included in Appendix A identify the receptors where potential glare may be visible.

Table 3-1: Summary of Results

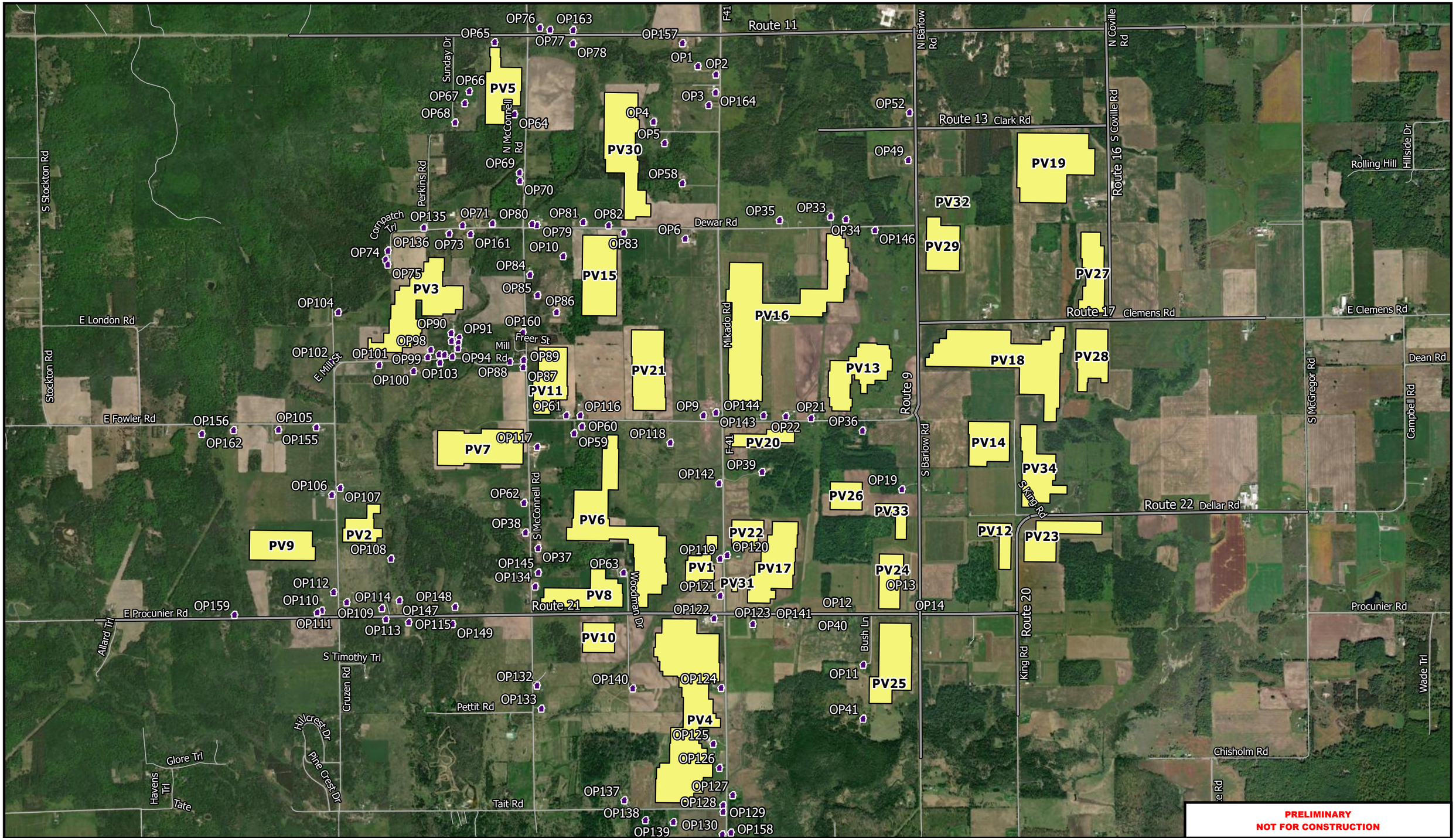
Type of Receptor	No. of Receptors	No. of Instances of "Yellow Glare"	
		Inconsequential	Consequential
Residences	32	0	0
Roads	8	1	0

The following summarizes key observations from the results of the Study:

- One of the 40 identified receptors is estimated to receive potential “yellow” glare. An instance of “yellow” glare is considered inconsequential if the glare is not visible at the receptor or the glare occurs from the same direction as the sun during sunrise or sunset.
    - The one instance of “yellow” glare is associated with PV 29 and occurs along Route 9.
    - However, the potential for glare occurs within an hour of sunrise and from a similar direction as the sun for the observer; because the sun is significantly more intense than estimated glare from the Project, the potential reflected glare is masked by the sun.
    - Nevertheless, operational controls will adjust the angle of the PV panels to negate any glare contribution.

The Study was performed using a conservative modeling approach with Project Site-specific conditions. Further, the Project Site was modeled with sunny conditions, complete coverage of PV panels in the modeled arrays, a flat horizon, and a terrain between the Project Site and the receptors. Due to the conservative approach of the Study, the actual duration and intensity of glare experienced at each receptor is expected to be less than those reported in the Study.

APPENDIX A – GLARE INTENSITY MAP



LEGEND

- Array
- Township
- Observation Point: No Glare
- Observation Point: Yellow Glare
- Route: No Glare
- Route: Yellow Glare

REFERENCE

0 0.5 1 MILES

0 0.45 0.9 KILOMETERS

N

MI ON

PRELIMINARY
NOT FOR CONSTRUCTION

Gustin Solar Energy Center
Solar Glare Study

LOCATION:	Harrisville Township, Alcona County, Michigan
CLIENT:	Consumers Energy Company
PROJ. NO.:	192088
CREATED:	09/29/2026

BURNS McDONNELL
www.burnsmcd.com

COPYRIGHT © 2022 BURNS & McDONNELL ENGINEERING COMPANY, INC. | PROPRIETARY & CONFIDENTIAL

APPENDIX B – GLARE RESULTS BY RECEPTOR

Table B-1: Glare Results by Receptor – Residences

Receptor Name	Latitude	Longitude	Daily Yellow Glare Duration (minutes)	Time of Day (EST)	Time of Year	Sunrise/Sunset[1]	Consequential
OP-7	44.606	-83.402	0	-	-	-	-
OP-8	44.607	-83.397	0	-	-	-	-
OP-15	44.613	-83.401	0	-	-	-	-
OP-16	44.612	-83.402	0	-	-	-	-
OP-17	44.613	-83.393	0	-	-	-	-
OP-18	44.611	-83.397	0	-	-	-	-
OP-20	44.622	-83.402	0	-	-	-	-
OP-23	44.611	-83.391	0	-	-	-	-
OP-24	44.620	-83.397	0	-	-	-	-
OP-25	44.620	-83.397	0	-	-	-	-
OP-26	44.620	-83.388	0	-	-	-	-
OP-27	44.635	-83.396	0	-	-	-	-
OP-28	44.635	-83.390	0	-	-	-	-
OP-29	44.634	-83.389	0	-	-	-	-
OP-30	44.634	-83.391	0	-	-	-	-
OP-31	44.644	-83.402	0	-	-	-	-
OP-32	44.646	-83.402	0	-	-	-	-
OP-42	44.607	-83.394	0	-	-	-	-
OP-43	44.620	-83.382	0	-	-	-	-
OP-44	44.621	-83.379	0	-	-	-	-
OP-45	44.620	-83.377	0	-	-	-	-
OP-46	44.635	-83.375	0	-	-	-	-
OP-47	44.643	-83.383	0	-	-	-	-
OP-48	44.645	-83.382	0	-	-	-	-

[1] Sunrise/Sunset column summarizes if the glare occurs within an hour of sunrise or sunset and from a similar direction as the sun. Since the intensity of the sun is significantly larger than the intensity of the glare from the Project, the impact of glare on the observer is negligible compared to the sun during the instance of glare.

Receptor Name	Latitude	Longitude	Daily Yellow Glare Duration (minutes)	Time of Day (EST)	Time of Year	Sunrise/Sunset[1]	Consequential
OP-50	44.648	-83.402	0	-	-	-	-
OP-51	44.649	-83.401	0	-	-	-	-
OP-53	44.651	-83.402	0	-	-	-	-
OP-54	44.649	-83.391	0	-	-	-	-
OP-55	44.650	-83.392	0	-	-	-	-
OP-56	44.650	-83.388	0	-	-	-	-
OP-57	44.650	-83.383	0	-	-	-	-
OP-150	44.641	-83.382	0	-	-	-	-

Table B-2: Glare Results by Receptor – Roads

Receptor Name	Associated Road	Daily Yellow Glare Duration (minutes)	Time of Day (EST)	Time of Year	Sunrise/Sunset[2]	Consequential
Route 9	S Barlow Road	5	8:15 AM – 8:45 AM	December	Yes	No
Route 11	Hwy 72	0	-	-	-	-
Route 13	Clark Rd	0	-	-	-	-
Route 16	S Coville Rd	0	-	-	-	-
Route 17	Clemens Rd	0	-	-	-	-
Route 20	King Rd	0	-	-	-	-
Route 21	E Procunier Road	0	-	-	-	-
Route 22	Dellar Rd	0	-	-	-	-

[2] Sunrise/Sunset column summarizes if the glare occurs within an hour of sunrise or sunset and from a similar direction as the sun. Since the intensity of the sun is significantly greater than the intensity of the reflected glare from the PV panels, the impact on the observer is negligible compared to the sun during the instance of glare.

Appendix C - FORGESOLAR METHODOLOGY UPDATE

Methodology Update Bulletin

ForgeSolar Radiometric Physics Engine v3.2.1 — July 2026
Document generated 29 Sep 2026

This bulletin summarizes recent updates to the ForgeSolar Radiometric Physics Engine, the radiometric modeling engine used by ForgeSolar for solar glare hazard analysis. These updates reflect advancements in optical physics research and improve the accuracy and safety compliance of glare assessments. Updates are grouped below by release, most recent first.

v3.2.1 (July 2026)

Single-Axis Tracker Footprint Orientation Refinement

For single-axis tracking systems using shade-avoidance or interval backtracking, the tracker's along-axis tilt is inferred from the orientation of the PV array's planar footprint. For footprints whose vertices spanned uneven terrain, the footprint orientation is now derived consistently from the planarized footprint. Fixed-mount arrays, and tracking systems on level footprints, are unaffected; reported footprint areas are unchanged for planar footprints and may increase slightly for footprints drawn across uneven terrain. As recommended, footprints spanning varying slopes or very uneven ground are often best modeled as separate planar arrays.

v3.2.0 (June 2026)

1. Route and Flight Path Downward View Restriction Correction

The downward view restriction filter for route and flight path receptors widened its threshold by half the beam spread, so that glare whose beam disk partially entered the observer's field of view was retained. At grazing sun angles (near sunrise and sunset) this allowed glare

originating below the path to slip past a 0° downward view restriction. Downward view restrictions of 1° or less are now treated as strict cutoffs, with no beam-spread allowance. Behavior for restrictions greater than 1° is unchanged.

2. Configurable Minimum Luminance Threshold and Sun Dominance Angle

The minimum luminance threshold and the sun dominance maximum angle are now user-configurable analysis inputs, set at the project level with an optional per-site override. Defaults are unchanged (5 000 cd/m^2 and 10°), so analyses run with default settings produce identical results to v3.1.3. The values used are recorded at analysis time and displayed on results pages and PDF reports.

3. Partial Obstruction Blocking for Route and Flight Path Receptors

Obstructions that partially block the line of sight between a PV array and a route or flight path now more accurately reduce the reported glare. This aligns route and flight path behavior with Observation Point receptors, which already modeled more accurate partial blocking. Hotspot plots for these receptors now show only the visible portion of the glare region. Results for sites without obstructions are unchanged.

v3.1.3 (May 4, 2026)

1. Vertical Surface Obstruction Pre-Filter Correction

The Vertical Surface (VS) analysis pipeline applies a coarse axis-aligned bounding box (AABB) pre-filter to skip obstructions that cannot affect the analysis before running the triangle-level line-of-sight check. In prior versions this pre-filter sometimes dropped obstructions between the VS and receptor(s) that were far from the VS.

2. Route and Flight Path Hotspot Plot Correction

The PV hotspot plot for route and flight path receptors sometimes failed to render the full remainder of each glare projection. The plot now displays the corrected glare projections, matching the inputs used for subtended-angle and retinal-irradiance computations. Annual glare minutes and hazard categories are unaffected.

v3.1.2 (March 2026)

1. Route Obstruction Mitigation

Enhanced obstruction mitigation for long route segments. Long route segments are now subdivided during the obstruction comparison so that each portion receives independent obstruction evaluation.

v3.1.1 (March 2026)

1. Sun Dominance Mitigation Correction

The sun dominance mitigation filter, which excludes glare timesteps where the reflected beam is within approximately 10 degrees of the direct sun from the observer's perspective, is now applied only to stationary observation point (OP) receptors. In prior versions, the filter was applied globally to all receptor types, including flight paths and routes. This was inconsistent with the German LAI policy, which defines sun dominance as a mitigation applicable only to fixed observation points. Flight path and route receptors now receive unfiltered glare results regardless of the sun dominance setting. Projects with sun dominance mitigation enabled should be re-analyzed to obtain updated results for path-based receptors.

v3.1.0 (March 2026)

1. Receptor Illuminance Calculations

The engine now computes receptor illuminance (lux) alongside source luminance (cd/m²) at each glare timestep. Luminance describes how bright the glare source appears, while illuminance describes how much light arrives at the receptor. Illuminance is derived from the existing per-timestep luminance and subtended angle data using the fundamental photometric relationship:

$$E_v = L \times \Omega_{source}$$

Where L is the source luminance and Ω_{source} is the solid angle of the glare source as seen from the receptor. This quantity requires no new physics inputs and is computed from data already produced at each timestep. Peak illuminance values are reported per receptor and per surface, providing an additional metric for assessing glare impact at observation points.

v3.0.0 (February 2026)

1. Improved Luminance Calculations

The engine now uses more physically accurate luminance calculations developed from independent laboratory measurements of commercial PV modules. Previous engine versions lacked direct luminance measurements and had to extrapolate values from slope-error data and simulated scaling, which in many cases yielded artificially low predictions.

1a. Product-Specific Profiles (BRDF-Based)

Product-specific profiles derive peak luminance directly from laboratory BRDF (Bidirectional Reflectance Distribution Function) characterization of commercial PV modules, performed by independent testing laboratories (e.g. Fraunhofer ISE) following established photometric standards (ASTM E2387). The measured luminance data provides piecewise maximum luminance (L_{max}) values as a function of incidence angle, and the engine evaluates these curves directly. This is the most physically accurate approach, as it uses empirically measured luminance from the actual module surface.

The generic "deeply textured" luminance curve is derived from the upper envelope (the maximum at each incidence angle) of three measured deeply-textured product profiles, with a ~15% safety margin applied. This ensures the generic deeply-textured profile is conservative relative to all known deeply-textured modules.

1b. Revised Generic Profiles (Radiometric Formula)

For revised generic profiles where product-specific BRDF data is not available, luminance is computed using the fundamental radiometric relationship for a reflecting surface:

$$L = E_v \times \rho / \Omega \times k_{peak}$$

Where:

- L is the source luminance (cd/m²)
- E_v is the illuminance on the panel surface (lux), derived from the direct normal irradiance (DNI)
- ρ is the surface reflectance at the given incidence angle

- Ω is the solid angle of the reflected beam cone (sr), computed from the beam divergence angle (β) as $\Omega = 2\pi(1 - \cos(\beta/2))$
- k_{peak} is a Gaussian beam peak correction factor (= 4.0) that converts from average cone luminance to the peak on-axis luminance an observer at beam center would experience, accounting for the non-uniform intensity distribution of the reflected beam

This formulation follows from first principles of radiometry and photometry. Key references include Palmer & Grant, 2010 ("The Art of Radiometry," SPIE Press); McCluney, 2014 ("Introduction to Radiometry and Photometry," 2nd ed., Artech House); and Boyd, 1983 ("Radiometry and the Detection of Optical Radiation," John Wiley & Sons). The BRDF measurement methodology follows Nicodemus et al., 1977 (NBS Monograph 160) and ASTM E2387.

In practice, the updated profiles may predict higher luminance values than the originals for the same site configuration. This reflects improved physical accuracy rather than a change in actual glare risk.

2. Beam Divergence Limit for Diffuse Surfaces

A 120° maximum beam divergence (β) is applied during the glare check calculation. This limit ensures physically meaningful results for highly diffuse PV surfaces, including newer product-specific modules with large slope error or surface roughness. Surfaces where the computed divergence exceeds this threshold are noted in the analysis results.

3. Unified PV and Vertical Surface Analysis Pipeline

The Vertical Surface (VS) and PV array glare analysis pipelines have been consolidated into a single shared methodology. VS analysis now uses the same parametric modeling approach as PV array analysis, providing deterministic glare prediction across both surface types. VS faces are mapped to a horizontal reference plane using coordinate rotation, enabling the full glare check used for PV arrays. This produces more accurate glare predictions and ensures consistent behavior for material profiles, beam divergence handling, and field-of-view filtering across both PV arrays and Vertical Surfaces.

4. Vertical Surface Obstruction Modeling

Vertical Surface analyses now fully model obstruction mitigation, matching the existing capability for PV array analyses. The obstruction mitigation cache is computed once per VS face and applied to all receptor types, using the same projection and intersection logic as PV arrays.

5. 3D Quad-Ray Intersection for Obstruction Mitigation

Obstruction mitigation has been upgraded to use a 3D quad-ray intersection approach. Each obstruction wall segment is decomposed into triangle pairs, and line-of-sight rays from PV surface sample points to receptor positions are tested against these triangles. This replaces the prior projection-based shadow approach, which relied on heuristic cone expansion and polygon subtraction. The new method directly answers the physical question of whether an obstruction blocks the line of sight between a PV surface and a receptor, producing more accurate and geometrically robust blocking predictions.

> ***Conclusion:*** *The results presented in current ForgeSolar reports represent a higher degree of accuracy and safety compliance than prior engine versions. The updates described above improve luminance modeling, extend analysis capabilities to Vertical Surfaces, and align the radiometric methodology with current optical safety research.*

© 2026 Sims Industries d/b/a ForgeSolar. All Rights Reserved.
For questions regarding this methodology update, contact support@forgesolar.com.



1898andco.com